Macromolecular Research, Vol. 23, No. 2, pp 145-148 (2015)
DOI 10.1007/s13233-015-3026-0

www.springer.com/13233
pISSN 1598-5032 eISSN 2092-7673

Directional Step Flow Across Ridges on Multiscale Two-Face Prism Array

Hyunsik Yoon*[,1], Seung Hyun Sung[2], Jai Hyun Koh[2], Sang Moon Kim[3], Se-Jin Choi[4], Kahp Y. Suh[3], and Kookheon Char*[,2]

[1]Department of Chemical and Biomolecular Engineering, Seoul National University of Science & Technology, Seoul 139-743, Korea
[2]School of Chemical and Biological Engineering, The National Initiative Creative Research Center for Intelligent Hybrids, The WCU Program for Chemical Convergence for Energy and Environment, Seoul National University, Seoul 151- 744, Korea
[3]School of Mechanical and Aerospace Engineering, Seoul National University, Seoul 151-744, Korea
[4]MCNet Co., Ltd., Room 307-1 Building 103 SK Ventium, Dangjeong-dong, Gunpo-si, Gyeonggi 435-833, Korea

Received July 21, 2014; Revised November 23, 2014; Accepted November 23, 2014

Abstract: Directional wetting or spreading on asymmetric structures have received much attention because of their potential to control the liquid flow in microfluidic devices. Although there have been many reports on directional liquid flows, the flow speeds of the directional flows could not be predicted. Here, we present a controllable strategy for directional flow on a multiscale two-face prism array, one face is smooth and the other face is roughened. The polymeric surface of the prism is roughened by oxygen plasma while the other side is blocked by a coated metal film. With the designed structure, we demonstrate a unidirectional liquid flow and manipulate the flow speed in an open channel. From a simplified model suggested here, the flow speed could be predicted quantitatively.

Keywords: prism, directional flow, polymer, microfluidics, contact angle.

Introduction

Recently, directional liquid flow[1-7] has received much attention for its potential uses to control liquid in microfluidics and water harvesting. To generate directionality in liquid flow on a given structure, the structures should have asymmetry. Among those attempts for the unidirectional wetting, bent or slanted pillar arrays should be good candidates for the directional wetting.[1,2] Although many groups have explained the directionality of liquid flow on asymmetric pillar structures, unfortunately, there are few attempts to control the flow speed quantitatively. Here, we present a unique multiscale structure for manipulation of liquid flow in an open channel. The structure is an array of triangular micro-prisms, one face of which is smooth while the other face has nanoscale roughness in multiscale two-face prism array. With the designed structure, we demonstrate a unidirectional liquid flow on an open channel. To investigate the unidirectional flow rate across the ridges of channels, we compared the speed of the directional flows with different channel widths. A simplified model presented in this paper explains the liquid movements in a good agreement with the experimental data.

*Corresponding Authors. E-mails: khchar@plaza.snu.ac.kr or hsyoon@seoultech.ac.kr

Experimental

Materials. The UV-curable prepolymer used for the prism array was a homogeneous liquid mixture of multi-functional acrylated prepolymer (ethoxylated trimethylolpropane triacrylate, M3130, Miwon Specialty Chemical Co., Ltd.) and acrylated-functionalized polysiloxane (Ac-PSi) (Silicon polyether acrylate, Rad2200N, Degussa). Additionally, Darocur 1173 (2-hydro-2-methyl-1-phenyl-1-propane, Ciba Specialty Chemicals, Switzerland) was simply blended as a photoinitiator with the homogeneous mixture of prepolymers for UV curability at 5 wt% with respect to the total amount of the blend of Ac-PSi and acrylated prepolymer.[8]

Fabrication of Prism Arrays. The master was prepared by mechanical machining. After the preparation of the master, drops of the homogeneous liquid mixture of acrylated prepolymer and acrylated-functionalized polysiloxane (Ac-PSi) with a photoinitiator were dispensed onto the master mold and a flexible PET (polyethylene terephthalate) film as a supporting plane was placed on top of the liquid mixture and lightly pressed. The prepolymers were then exposed to ultra-violet (UV) light (λ= 250~400 nm) for several seconds (dose=100 mJcm^{-2}) through the backside of the transparent PET film for solidification by crosslinking between acrylate functional groups. Then, the cured polymer mixture on the PET film was removed from the master.

Oblique Metal Deposition. The polymer prism array (50 μm in period, 45° in the prism angle) was coated with 20 nm thick gold metal only on one side of the prism by oblique metal evaporation (Two-face prism array). We used a thermal evaporator for the metal deposition and placed the polymer prism array on an inclined holder with an angle around 50°. During the deposition, evaporated metal atoms were guided down vertically at ~ 10^{-6} Torr, with the inclined holder defining the oblique incidence angle, resulting in the deposition of metal layers only on one side of the prism array.

Selective Etching by Oxygen Plasma. Subsequently, the two-face prism array was etched by oxygen plasma. The polymer face was etched selectively while the silicon-containing part acted as an etch barrier in the form of silicon oxide (SiOx) during the oxygen plasma etching. The metal-covered face was not etched because the metal layer blocked the etching by oxygen plasma. After etching, we obtained hierarchical two-face prism arrays, with symmetry in microscale but asymmetry in nanoscale. The oxygen plasma etching (RIE 80 plus, Oxford instrument) was carried out at 50 mTorr of total gas pressure, 10 standard cubic centimeters (sccm) of oxygen gas flow rate and 200 W of RF power.

Measurements. High-resolution scanning electron microscopy (SEM) images were obtained using Philips XL30FEG. To avoid charging effects, the polymer prism film was sputter coated 5 nm thick with platinum prior to measurements.

Results and Discussion

Figure 1 schematically shows the procedure involved in fabricating the multiscale two-face prism array. A polymer replica consisting of silicon-containing acrylated polysiloxane (Ac-PSi) and acrylated prepolymer was made from the original master that had been prepared by mechanical machining.[8] To prepare the asymmetric two-face prism array, an Au film was coated only on one face of the prism by oblique deposition.[7,9-11] After the metal coating, one face remains polymeric while the other is metal-coated, resulting in a two-face prism array.

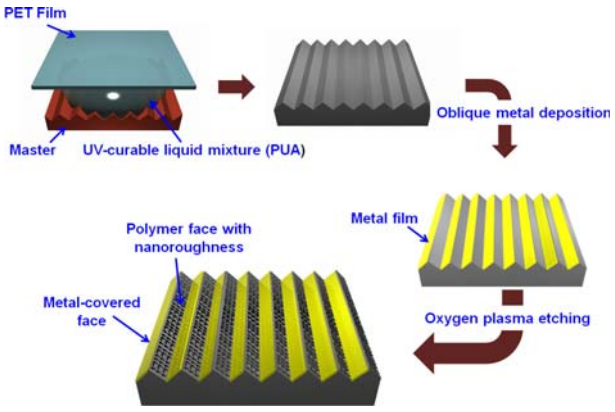

Figure 1. A schematic illustration for the fabrication of a multiscale two-prism array.

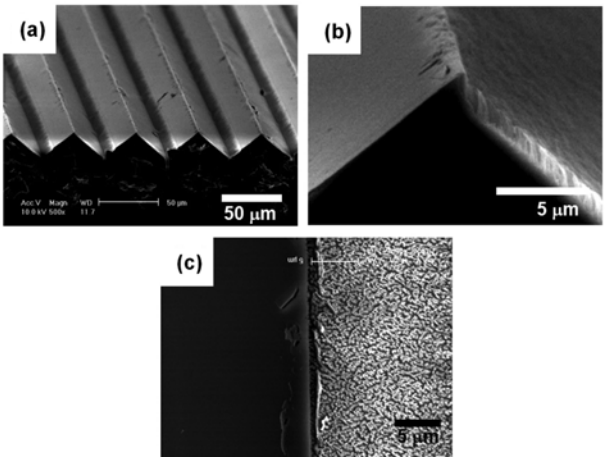

Figure 2. (a) A SEM image of a prism array showing the symmetry in microscale. (b) A magnified SEM image of the prism showing the asymmetry in nanoscale. (c) A plane-view of a SEM image of the prism showing the metal-deposited smooth surface (left) and the roughened polymeric surface (right) derived from oxygen plasma treatment.

To magnify the difference in wetting characteristics, roughness was selectively induced on the polymer face by oxygen plasma etching. During the etching process, the polymer domain sides spontaneously became roughened as a result of the hard-masking role of Ac-PSi domains. The detailed mechanism of roughening process by oxygen plasma etching has been presented elsewhere.[8]

Figure 2 shows scanning electron microscope (SEM) images of the multiscale two-face prism arrays presented here. As seen from Figure 2(a), the period is 50 μm with a prism angle of 45° at both sides. Magnified views in Figure 2(b)-(c) demonstrate that the prism has the symmetry in microscale and the asymmetry in nanoscale at the same time: one face is covered with a metal film while the other is a polymer surface with rough domains of < 150 nm in width and ~1 μm in depth. The geometry of the roughened surface could be controlled by adjusting etching time and other process parameters.[8]

To demonstrate directional liquid flow on the multiscale two face prism array, we placed a water droplet on the structure and increased the liquid volume at a constant feeding rate. Figure 3(a) shows the movie cuts of unidirectional liquid flow on the designed surface. It is noted that the water front moves unidirectionally toward the roughened polymer surface. The movie cuts of unidirectional liquid flow against gravity are shown in Figure 3(b). As our previous work described,[7] the marching liquid-front is pinned at the channel ridge and the pinning is held even in increasing liquid volume until the contact angle of the liquid-front reaches its critical angle at the edge.[12,13] The critical contact angle θ_c can be written as follows:[12,13]

$$\theta_c=\theta+\alpha \quad (1)$$

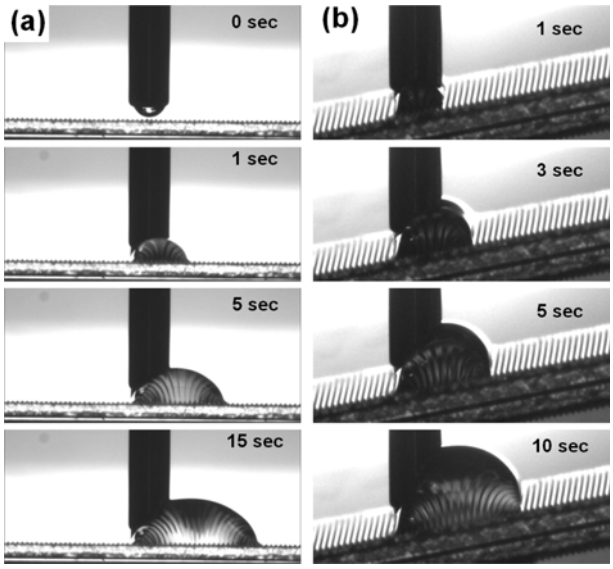

Figure 3. (a) Movie cuts of a liquid flow on the multiscale two-face prism array. (b) Movie cuts of a liquid flow against gravity on the multiscale two-face prism array.

where θ is the equilibrium contact angle on a planar surface or the intrinsic contact angle and α is the angle subtended by the two prism surfaces forming a solid edge, which is referred to as the edge angle. In the two-face prism system, the critical contact angles of the two-faces are different from each other because of their different surface properties and morphologies. As a result, the critical contact angle is higher on the smooth surface (the left faces of the prism array) than the roughened surface after oxygen plasma etching and the liquid front is guided to move in the direction of lower critical angle (the right, roughened polymer faces) as the liquid volume is increased. After the oxygen plasma etching to make nanoroughness, the entire prism surface becomes hydrophilic. Moreover, the highly roughened polymer face shows superhydrophilicity in accordance with the Wenzel's model.[14-17] By the repetition of stepping liquid movement, the water front moves toward the lower critical angle in a step-wise fashion.

To investigate the step flows across the ridges of channels, we compared the directional liquid flows with different channel widths. Figure 4(a) shows movie cuts of liquid flow with a channel width of 4 mm. At the first stage, the liquid flows along the V-shape ridges. After reaching the edges of the open channel, the liquid starts to move across the ridges. On an open channel with a width of 1.5 mm, on the other hand, the flow speed becomes faster (Figure 4(b) compared to that on the wide channel.

With the geometry of prism array given in Figure 5, the liquid volume is calculated as a function of several parameters, such as width and period of prism array, prism angle, and the lowest critical contact angle. With a simple calculation based on geometry, the relation is given by:

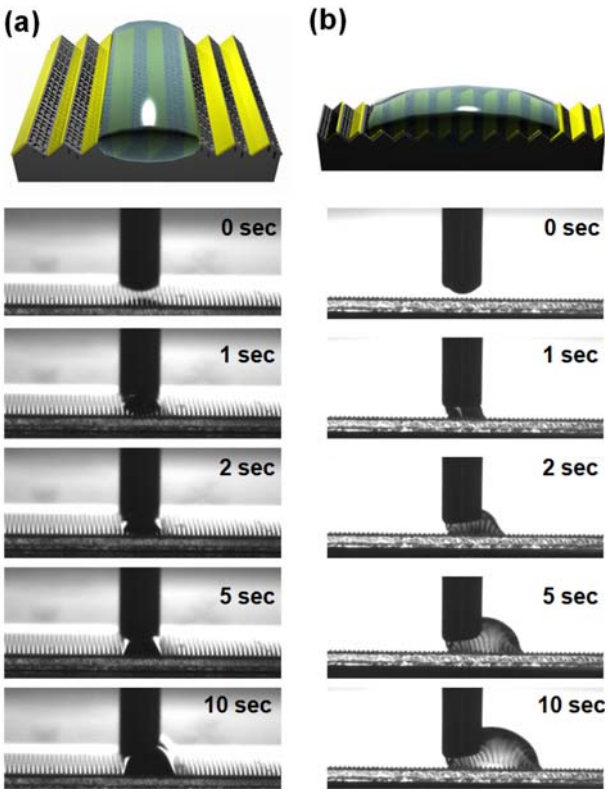

Figure 4. (a) Movie cuts of a liquid flow on an open channel in a channel width of 4 mm. (b) Movie cuts of a liquid flow on an open channel in a channel width of 1.5 mm.

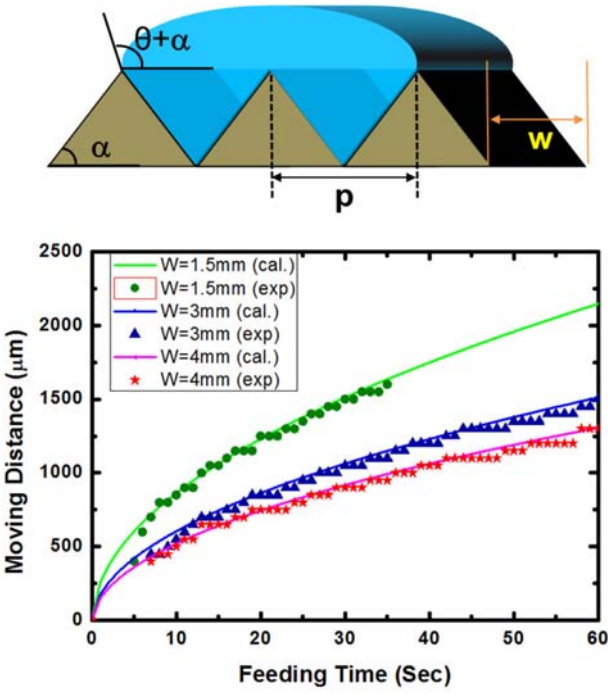

Figure 5. A scheme showing prism parameters to control liquid flow and the comparison between theory (eq. (2)) and experimental data.

$$V = \left[\frac{1}{4}n\tan\alpha + \frac{n^2(2(\theta+\alpha)+\sin 2(\theta+\alpha))}{4(1-\cos 2(\theta+\alpha))}\right]p^2 W \quad (2)$$

where n is the number of prisms wetted by a water droplet, θ is the equilibrium contact angle on a planar surface, α is the prism angle (45°), p is the period of prism (50 μm), W is the width of prism array (three different widths of 1.5 mm, 3 mm, 4 mm were used in the experiments), and V is the liquid volume. After going through algebraic manipulations, one can derive an equation for the lateral movement of liquid, which is written by:

$$np = (\sqrt{4AV/W + p^2B^2} - pB)/2A \quad (3)$$

where $A = \frac{2(\theta+\alpha)+\sin 2(\theta+\alpha)}{4(1-\cos 2(\theta+\alpha))}$ and $B = \frac{1}{4}\tan\alpha$.

Shown in Figure 5 are the comparisons between the distances travelled by water front as predicted by the equation given above and the actual experimental data as a function of feeding time. Note that the liquid volume is simply given by the feeding time multiplied by the injection rate of a droplet. As can be seen from the figure, the actual liquid movement is in excellent agreement with the law of conservation of mass for three different channel widths of 1.5, 3, and 4 mm. Here, the equilibrium contact angle of 30° was used throughout the calculation. It is also noted that we neglect the effect of the volume of the needle for simplification, which induced the deviation at the early stage of the movement in the graph.

Conclusions

In summary, we designed and fabricated periodic, multiscale two-face prism arrays one face is smooth while the other face is roughened. It was observed that the liquid flows in the direction of the lower critical contact angle. A simple model was derived to predict the flow speed as a function of prism geometry in good agreement with the experimental results. The concept of step flow on the multiscale two-face prism arrays could be controllable for flow rate on open channels.

Acknowledgments. This work was financially supported by the National Creative Research Initiative Center for Intelligent Hybrids (No. 2010-0018290) through the National Research Foundation of Korea (NRF) grants, the Basic Science Research Program (2012R1A1A1013688, 2013R1A2A2A04015981), and the BK21 Programs funded by the Ministry of Education, Science and Technology (MEST) of Korea.

References

(1) K.-H. Chu, R. Xiao, and E. N. Wang, *Nat. Mater.*, **9**, 413 (2010).
(2) T.-I. Kim and K. Y. Suh, *Soft Matter*, **5**, 4131 (2009).
(3) N. A. Malvadkar, M. J. Hancock, K. Sekeroglu, W. J. Dressick, and M. C. Demirel, *Nat. Mater.*, **9**, 1023 (2010).
(4) S. Daniel, S. Sircar, J. Gliem, and M. K. Chaudhury, *Langmuir*, **20**, 4085 (2004).
(5) Y. Zheng, H. Bai, Z. Huang, X. Tian, F.-Q. Nie, Y. Zhao, J. Zhai, and L. Jiang, *Nature*, **463**, 640 (2010).
(6) M. Prakash, D. Quéré, and J. W. Bush, *Science*, **320**, 931 (2008).
(7) S. M. Kim, D. H. Kang, J. H. Koh, H. S. Suh, H. Yoon, K.-Y. Suh, and K. Char, *Soft Matter*, **9**, 4145 (2013).
(8) S.-J. Choi, M. K. Choi, D. Tahk, and H. Yoon, *J. Mater. Chem.*, **21**, 14936 (2011).
(9) H. Yoon, S.-G. Oh, D. S. Kang, J. M. Park, S. J. Choi, K. Y. Suh, K. Char, and H. H. Lee, *Nat. Commun.*, **2**, 455 (2011).
(10) H. Yoon, H. E. Jeong, T.-I. Kim, T. J. Kang, D. Tahk, K. Char, and K. Y. Suh, *Nano Today*, **4**, 385 (2009).
(11) Y. Choi, S. Hong, and L. P. Lee, *Nano Lett.*, **9**, 3726 (2009).
(12) J. Oliver, C. Huh, and S. Mason, *J. Colloid Interface Sci.*, **59**, 568 (1977).
(13) F.-M. Chang, S.-J. Hong, Y.-J. Sheng, and H.-K. Tsao, *J. Phys. Chem. C*, **114**, 1615 (2010).
(14) D. Quéré, *Annu. Rev. Mater. Res.*, **38**, 71 (2008).
(15) N. Verplanck, Y. Coffinier, V. Thomy, and R. Boukherroub, *Nanoscale Res. Lett.*, **2**, 577 (2007).
(16) E. Ueda and P. A. Levkin, *Adv. Mater.*, **25**, 1234 (2013).
(17) S. Nishimoto and B. Bhushan, R. *Soc. Chem. Adv.*, **3**, 671 (2013).